Anisotropic magnetoresistance and spin polarization of $La_{0.7}Sr_{0.3}MnO_3/SrTiO_3$ superlattices

L. M. Wang and Chih-Chian Guo
Department of Electrical Engineering, Da-Yeh University, Chang-Hwa 515, Taiwan

(Received 3 June 2005; accepted 30 August 2005; published online 17 October 2005)

The crystalline structure, anisotropic magnetoresistance (AMR), and magnetization of $La_{0.7}Sr_{0.3}MnO_3/SrTiO_3$ (LSMO/STO) superlattices grown by a rf sputtering system are systematically analyzed to study the spin polarization of manganite at interfaces. The presence of positive low-temperature AMR in LSMO/STO superlattices implies that two bands of majority and minority character contribute to the transport properties, leading to a reduced spin polarization. Furthermore, the magnetization of superlattices follows the $T^{3/2}$ law and decays more quickly as the thickness ratio d_{STO}/d_{LSMO} increases, corresponding to a reduced exchange coupling. The results clearly show that the spin polarization is strongly correlated with the influence of interface-induced strain on the structure. © *2005 American Institute of Physics*. [DOI: 10.1063/1.2112167]

Manganites of the type $R_{1-x}A_xMnO_3$ (R=rare earth, A=Ca, Sr, Ba, and Pb) are considered to be half-metallic and, therefore, ideal candidates for the use in spin-electronic devices.[1] Recently, a tunneling magnetoresistance (TMR) ratio of more than 1800% at 4 K for $La_{2/3}Sr_{1/3}MnO_3/SrTiO_3/La_{2/3}Sr_{1/3}MnO_3$ trilayer junctions was obtained,[2] leading to an inferred electrode spin polarization of at least 95%. However, the reported low-field magnetoresistance for these manganite-based devices decreases rapidly with increased temperature, and even vanishes at temperatures well below the Curie temperature of bulk manganites. It is generally believed that tunneling is a mechanism occurring near the electrode/barrier interface, and the TMR is dominated by charge carriers near the interface boundary.[3,4] In particular, the rapid decrease of the spin polarization at interfaces with increasing temperature would thus limit the application of the half-metallic materials for spin-electronics devices. That points to an important issue in the physics of their interface properties. Ferromagnetic manganite-insulator superlattices, containing many interfaces of interest, offer the possibility to probe the properties of ultrathin manganite layers and the interface magnetism. Up to now, several groups have reported on the fundamental properties of $La_{1-x}A_xMnO_3/SrTiO_3$ (A=Ca, Sr, and Ba) superlattices.[5–8] The suppression in both T_C and magnetization accompanying an increase of resistivity as the thickness of $La_{0.7}Sr_{0.3}MnO_3$ (LSMO) layers decreases was observed.[5,6] Various magneto-transport properties of manganite-insulator superlattices have been attributed to the strain effect[7] or interlayer coupling.[8] However, for the ferromagnetic manganite-based superlattices, surprisingly few studies have so far been made on the central problem of the spin polarization in ultrathin manganite layers. This is a key issue for the fabrication of any spin-electronic device composed of manganite/insulator tunneling interfaces.

$La_{0.7}Sr_{0.3}MnO_3/SrTiO_3$ (LSMO/STO) superlattices grown on (001) $LaAlO_3$ substrate were prepared in a rf magnetron sputtering system as previously described.[9] A buffer $SrTiO_3$ (STO) layer of 60 nm in thickness was deposited prior to the growth of LSMO/STO superlattices to diminish the substrate-induced strain. The deposition was kept at the same growth conditions (grown at 720 °C with a sputtering pressure of 300 mTorr and an oxygen annealing before cooling process) to prevent the composition variation among the superlattices.

Figure 1 is a high-resolution cross-sectional transmission electron microscopy (TEM) lattice image of a LSMO/STO superlattice denoted by $(76/56)_{12}$ in [010] direction, where the numbers in parentheses correspond respectively to the thicknesses of LSMO and STO layers, and the subscript denotes the total repeated number of bilayers. This figure shows a perfectly epitaxial growth with sharp interfaces between LSMO and STO within less than 1 nm. The presented TEM image shows a more clearly coherent hetrostructure with sharp interfaces than that reported on LSMO/STO superlattices grown by pulsed laser deposition.[6] It also demonstrates that high-quality perovskite superlattices can be achieved by a lower-cost sputtering technique. Figure 2(a) shows the x-ray θ-2θ diffraction spectra in the region near

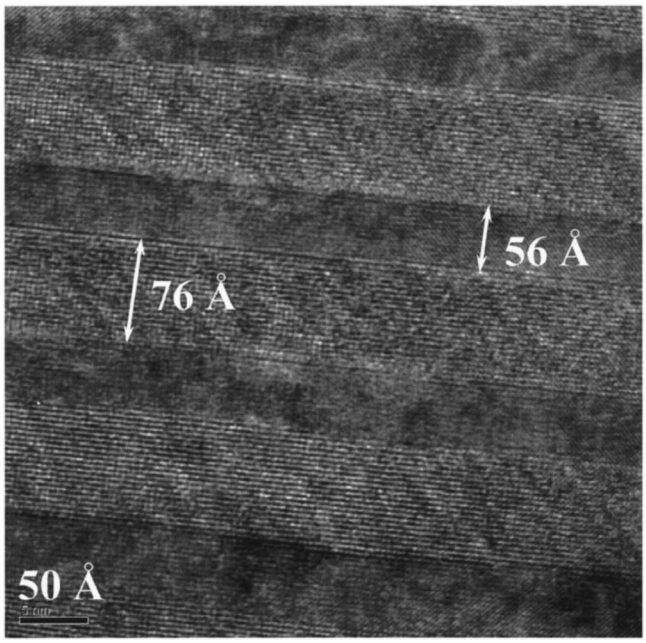

FIG. 1. High-resolution cross-sectional TEM lattice image of a LSMO/STO superlattice.

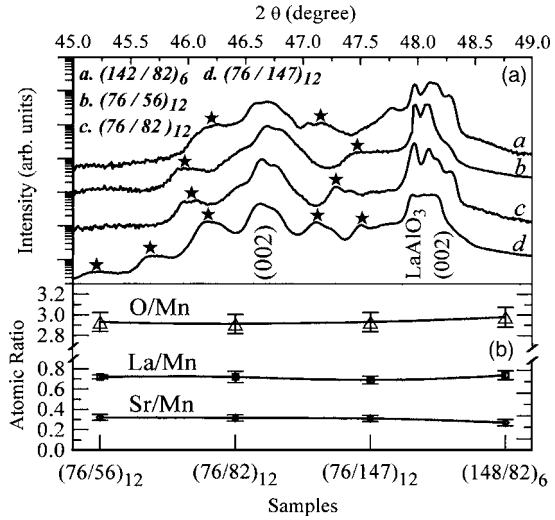

FIG. 2. (a) X-ray $\theta-2\theta$ diffraction spectra in the region near the (002) peak for a series of LSMO/STO superlattices. The satellite peaks are indicated by star symbols. (b) The atomic ratios of La/Mn, Sr/Mn, and O/Mn for the corresponding samples.

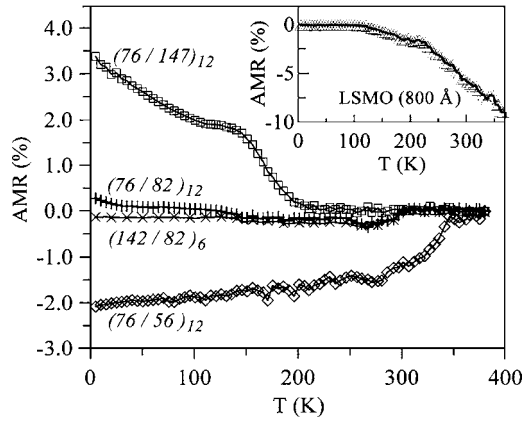

FIG. 3. Temperature dependence of AMR for a series of LSMO/STO superlattices. The inset shows the AMR behavior of the 800-Å LSMO film for comparison.

the (002) peak for a series of LSMO/STO superlattices. Clearly, the 2θ position of the (002) peak is dependent on the layer thickness in LSMO/STO superlattices, indicating a variation of out-of-plane strain among these superlattices.[7] For a superlattice with thicker STO layers or thinner LSMO layers, an enhanced *c*-axis lattice was observed. This feature is similar to that observed in LSMO/STO superlattices grown on STO substrates.[5] In Fig. 2(a), the presence of the satellite peaks on both sides of the main peak (002) confirms that a periodic structure in the superlattices has been achieved. The modulation wavelength, $\Lambda = d_{\mathrm{LSMO}} + d_{\mathrm{STO}}$, where d_{LSMO} and d_{STO} are the thickness of the LSMO and STO layers, respectively, can be calculated from the separation of two successive peaks (i and $i+1$) using the equation: $\Lambda = (\lambda/2) \times [1/(\sin\theta_i - \sin\theta_{i+1})]$, where λ is the x-ray wavelength ($\lambda = 1.5406$ Å). The modulation wavelength $\Lambda = 128$ Å obtained from the x-ray data for $(76/56)_{12}$ superlattice is in close agreement with that of 132Å observed in the TEM image. Figure 2(b) shows the atomic ratios of La/Mn, Sr/Mn, and O/Mn determined by an energy dispersive spectrometer (EDS) using an EMAX system detector attached to a Hitachi S-3000N scanning electron microscope for the corresponding samples shown in Fig. 2(a). Here the compositions contributed from the substrate and STO layers are subtracted to obtain the atomic ratios in LSMO layers. Clearly, the EDS analysis reveals that the dopant concentration changes very little and shows almost stoichiometric values for samples. The EDS result allows us to compare the physics properties between the stoichiometric superlattices with different lattice constants by taking account of the strain effect.

Figure 3 shows the temperature dependence of AMR for a series of LSMO/STO superlattices. The AMR is defined as $\mathrm{AMR}(7\ T) = \mathrm{MR}(7\ T)_{\parallel} - \mathrm{MR}(7\ T)_{\perp}$, where the magnetoresistance ratio (MR) is defined as $\mathrm{MR} = [\rho(H) - \rho(0)]/\rho(H)$, and $\mathrm{MR}(7\ T)_{\parallel}$ and $\mathrm{MR}(7\ T)_{\perp}$ denote the longitudinal ($H \parallel$ the electric current) and transverse ($H \perp$ the electric current) magnetoresistance ratio, respectively. Here the data were obtained with currents along crystal [100] direction, and magnetic fields applied in the film plane to eliminate the demagnetization effect. It is found that with decreasing d_{LSMO} or increasing d_{STO}, the value of resistivity ρ increases, and ρ reveals a metallic state at low temperatures with a maximum MR value occurring near the Curie temperature for all superlattices (not shown). In Fig. 3, it can be observed that the low-temperature AMR value increases gradually and changes to a positive value with decreasing d_{LSMO} or increasing d_{STO}. The top inset of Fig. 3 shows the AMR behavior of the 800-Å LSMO film for comparison. It presents a very similar feature compared to that of $La_{0.7}Ca_{0.3}MnO_3$ films observed by Ziese,[10] but a quit different behavior from that of the superlattices studied. The excess negative AMR near T_C for high-quality manganite films has been suggested to be related to the inhomogeneous magnetic state.[11] Moreover, contrary to the high-quality epitaxial films, the AMR, being highest at low temperatures with no clear peak near T_C, was also observed in a polycrystalline $La_{0.7}Ca_{0.3}MnO_3$ film.[10] Since the grain-boundary or interface-scattering resistance is isotropic and will be canceled in the calculation of the AMR, the anisotropic transport properties have been suggested to be related to the local lattice distortions of the Mn–O bonds.[11] Thus, the AMR reflects an intrinsic transport property and is related to the crystalline structure. This gives a good account for the variegated AMR behaviors observed in the stoichiometric LSMO/STO superlattices. It must be recalled here that a variation of out-of-plane strain can be deduced from the x-ray results, as previously mentioned. Turning now to concentrate on the low-temperature AMR features of LSMO/STO superlattices, Ziese has recently analyzed the AMR behaviors of $La_{0.7}Ca_{0.3}MnO_3$ and Fe_3O_4 films within the two-current model and an atomic *d*-state calculation.[10] For the $La_{0.7}Ca_{0.3}MnO_3$ film, in which a negative AMR was observed, he pointed out a weak influence of a minority spin band. Additionally, based on the observation of a positive AMR in the Fe_3O_4 film, it was suggested that at least two bands of majority and minority character contribute to the transport properties of Fe_3O_4, leading to its lower spin polarization. The same is true of the presented case for LSMO/STO superlattices. The presence of positive AMR in LSMO/STO superlattices with thinner LSMO layers or thicker STO layers implies a reduced spin polarization occurring in them.

To explore the temperature dependence of spin polarization P(T), a convenient method is to study the temperature dependence of magnetization M(T).[12,13] The measurement of

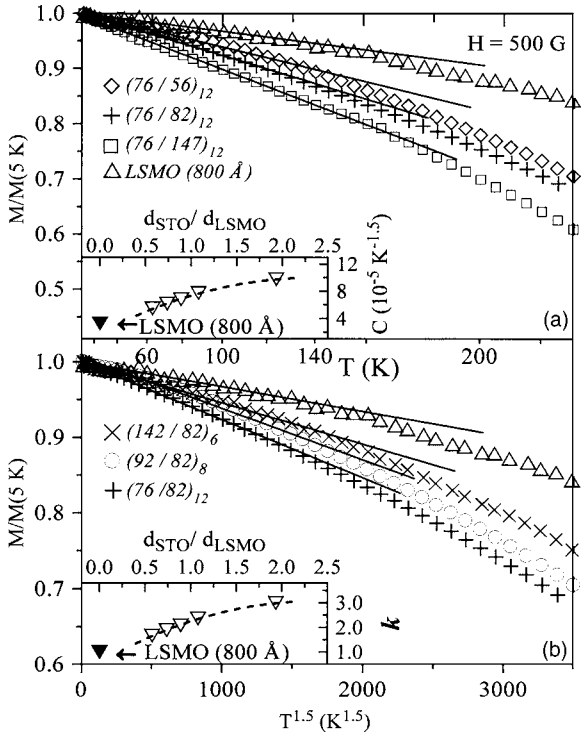

FIG. 4. Normalized magnetization M/M(5 K) measured with $H=500$ G as a function of $T^{3/2}$ for (a) a series of superlattices with varied thicknesses of STO layers and (b) a series of superlattices with varied thicknesses of LSMO layers. Inset of (a): the value of constant C as a function of $d_{\mathrm{STO}}/d_{\mathrm{LSMO}}$ ratio. Inset of (b): the parameter k as a function of $d_{\mathrm{STO}}/d_{\mathrm{LSMO}}$ ratio. The dashed lines are for the purpose of guiding the eye.

M(T) on LSMO/STO superlattices is supposed to reflect the P(T) over the ultrathin LSMO layers. The M(T), being proportional to P(T), should follow the $T^{3/2}$ law according to $M(T)/M(0)=1-CT^{3/2}=1-kC_{\mathrm{bulk}}T^{3/2}$, where C_{bulk} is the constant describing the decrease of the bulk magnetization due to thermal excitation of the spin wave, and $k=2$ for the ideal surface case.[14] Figures 4(a) and 4(b) show the normalized magnetization M/M(5 K) measured with $H=500$ G as a function of $T^{3/2}$ for two series of superlattices with varied thicknesses of STO layers and LSMO layers, respectively. It can be seen that the $M(T)$ follows the $T^{3/2}$ law at temperatures below 140 K for all the superlattices and the LSMO film. It can also be seen that the M(T) of superlattices decays more quickly with increasing temperature, corresponding to a fast decay of $P(T)$, as the STO layers become thicker or the LSMO layers become thinner. It is found that the value of constant C increases with an increase of $d_{\mathrm{STO}}/d_{\mathrm{LSMO}}$ ratio, as shown in the inset of Fig. 4(a). Taking $k=1$ for the LSMO film, the parameter k of superlattices also shows a monotonous increase with an increase of $d_{\mathrm{STO}}/d_{\mathrm{LSMO}}$ ratio, as seen in the inset of Fig. 4(b). The presented values of k, in the range of 1.5–3.0, are comparable to those in the range of 1.1–4.2 derived from the $P(T)$ of $La_{2/3}Sr_{1/3}MnO_3$ TMR devices.[13] It is noteworthy that the parameter k can be a measure of the exchange coupling $J_\perp$ on a path perpendicular to the interfaces.[12] According to Mathon,[15] the value of $k=3.0$ for the $(76/147)_{12}$ superlattice corresponds to $J_\perp/J \approx 0.3$, where J is the exchange interaction in the bulk. It is known that a reduced exchange coupling should not completely separate the majority carrier conduction band from the minority band, leading to an incomplete polarization of the carriers.[16] This result is consistent with the inference from the AMR properties previously discussed.

In summary, high-quality LSMO/STO superlattices have been prepared in a rf sputtering system, and characterized by the TEM image, x-ray diffraction, EDS analysis, and resistive measurement. These superlattices offer a good opportunity to probe the properties of ultrathin manganite layers and the interface magnetism. According to Ziese,[10] the presence of positive low-temperature AMR in LSMO/STO superlattices with thinner LSMO layers or thicker STO layers implies that at least two bands, of majority and minority character, contribute to the transport properties, leading to a reduced spin polarization. Furthermore, the $M(T)$ of superlattices follows the $T^{3/2}$ law at low temperatures and decays more quickly as the $d_{\mathrm{STO}}/d_{\mathrm{LSMO}}$ ratio increases. The results clearly show that the spin polarization is strongly correlated with the influence of interface-induced strain on the structure. The interface-induced strain must be taken into account in the fabrications of TMR devices based on doped manganites.

The authors thank the National Science Council of the Republic of China for financial support under Grant Nos. NSC 93-2112-M-212-001 and NSC 94-2623-7-212-003-AT. This work was also partially supported by Da-Yeh University under Grant No. ORD-9303.

[1] E. O. Wollan and W. C. Koehler, Phys. Rev. **100**, 545 (1955).
[2] M. Bowen, M. Bibes, A. Barthélémy, J.-P. Contour, A. Anane, Y. Lemaî tre, and A. Fert, Appl. Phys. Lett. **82**, 233 (2003).
[3] J.-H. Park, E. Vescovo, H.-J. Kim, C. Kwon, R. Ramesh, and T. Venkatesan, Phys. Rev. Lett. **81**, 1953 (1998).
[4] J. S. Moodera, J. Nowak, and R. J. M. van de Veerdonk, Phys. Rev. Lett. **80**, 2941 (1998).
[5] M. Sahana, T. Walter, K. Dörr, K.-H. Müller, D. Eckert, and K. Brand, J. Appl. Phys. **89**, 6834 (2001).
[6] K. Dörr, T. Walter, M. Sahana, K.-H. Müller, K. Nenkov, K. Brand, and L. Schultz, J. Appl. Phys. **89**, 6973 (2001).
[7] Y. Lu, J. Klein, C. Höfener, B. Wiedenhorst, J. B. Philipp, F. Herbstritt, A. Marx, L. Alff, and R. Gross, Phys. Rev. B **62**, 15806 (2000).
[8] M. Izumi, Y. Ogimoto, Y. Okimoto, T. Manako, P. Ahmet, K. Nakajima, T. Chikyow, M. Kawasaki, and Y. Tokura, Phys. Rev. B **64**, 064429 (2001).
[9] L. M. Wang, H. H. Sung, B. T. Su, H. C. Yang, and H. E. Horng, J. Appl. Phys. **88**, 4236 (2000).
[10] M. Ziese, Phys. Rev. B **62**, 1044 (2000); M. Ziese and S. P. Sena, J. Phys.: Condens. Matter **10**, 2727 (1998).
[11] V. S. Amaral, A. A. C. S. Lourenco, J. P. Araújo, P. B. Tavares, E. Alves, J. B. Sousa, J. M. Vieira, M. F. da Silva, and J. C. Soares, J. Magn. Magn. Mater. **211**, 1 (2000).
[12] D. Mauri, D. Scholl, H. C. Siegmann, and E. Kay, Phys. Rev. Lett. **61**, 758 (1988).
[13] V. Garcia, M. Bibes, A. Barthélémy, M. Bowen, E. Jacquet, J.-P. Contour, and A. Fert, Phys. Rev. B **69**, 052403 (2004).
[14] D. Mills and A. Maradudin, J. Phys. Chem. Solids **28**, 1855 (1967).
[15] J. Mathon, Physica B & C **149B**, 31 (1988).
[16] H. Y. Hwang, S-W. Cheong, N. P. Ong, and B. Batlogg, Phys. Rev. Lett. **77**, 2041 (1996).